Swelling behavior and gas permeation performance of PVAm/PVA blend FSC membrane

Liyuan Deng, May-Britt Hägg*

Department of Chemical Engineering, Norwegian University of Science and Technology (NTNU), NO-7491 Trondheim, Norway

ARTICLE INFO

ABSTRACT

Water swelling behavior and permeation performance of CO_2 and N_2, CH_4, H_2 in polyvinylamine/polyvinylalcohol (PVAm/PVA) blend fixed-site-carrier (FSC) membrane were studied with respect to the relative humidity of the gases in the separation system. Two exponential fittings were presented to describe the two stage swelling behavior of the membrane. The effects of operating parameters on CO_2 separation performance were investigated and optimized. Interactions between gases in mixed gas separation were discussed. Experiments showed exponential dependencies of gas permeance on relative humidity, which could be explained by the dependence of gas diffusion on membrane swelling and the unique CO_2 facilitated transport membrane in this membrane. The reversible hydration reactions of CO_2 initiated by amino carriers in the water swelling membrane facilitate the CO_2 transport. CO_2 diffuses in the form of HCO_3^- in this membrane, resulting in both high CO_2 permeance and selectivity over other gases. A selectivity up to 45 and CO_2 permeance up to $0.55\,m^3(STP)/(m^2\,h\,bar)$ for CO_2–CH_4 separation, and a selectivity up to 160 and CO_2 permeance up to $0.83\,m^3(STP)/(m^2\,h\,bar)$ for CO_2–N_2 separation were documented.

1. Introduction

The most commonly used technology for CO_2 capture today is chemical absorption; a technology with high capital cost, high energy consumption and potentially environmental pollution. Being environment-friendly, energy-saving, low-cost and with much smaller footprint, membrane separation is very well recognized as a promising green alternative to amine absorption process today. To make membrane separation competitive with amine absorption process, efficient membranes with both high CO_2 permeability and good selectivity in favor of CO_2 are required. Since being firstly reported in 1960, the facilitated transport membrane has come a breakthrough that can overcome the trade-off relationship between CO_2 permeance and selectivity [1–3]. Benefiting from the reversible reaction between CO_2 and carrier compounds, supported liquid membranes (SLMs) exhibit both high CO_2 permeance and CO_2/CH_4 selectivity. However, these membranes suffer from solution loss and deactivation of the complexing agent from the porous support, hence industrial application on a large scale is most likely not a choice. LeBlanc et al. firstly reported ion-exchange facilitated transport membranes to overcome the limitations of SLMs [4]. Since then great progress on developing facilitated transport

membranes with fixed-site-carriers (FSCs) has been made. With the carriers fixed chemically (covalently) or physically to a solid polymer matrix, fixed-site-carrier (FSC) membranes exhibit generally higher stability compared with SLMs.

In this work, a homogeneous polyvinylamine/polyvinylalcohol (PVAm/PVA) fixed-site-carrier membrane was prepared from the blending of the two hydrogels with desired membrane properties for CO_2 separation. PVAm has a high density of fixed primary amino groups as CO_2 transport carriers [5], in which the reversible reactions of CO_2 with amino carriers facilitate the CO_2 transport, resulting in high CO_2 permeability and selectivity. While the blending of PVAm with PVA, a mechanically robust polymer, enhances polymeric network with good membrane forming properties by the entanglement of the PVA chains with the PVAm chains [6–12], providing good membrane stability and mechanical strength. In addition, it has been confirmed that CO_2 transports through the water-swollen FSC membrane in the form of HCO_3^- and diffuse as ions in liquid [5,13,14]. The membrane is hence capable of combining the advantages of both supported liquid membrane and solid polymeric membrane, exhibiting higher CO_2 permeance than that of FSC membranes in dry states. Due to the unique facilitated transport mechanism which involves the water swollen in membrane, the swelling behavior of this FSC membrane shows crucial influences on the gas separation. Feng and co-workers elucidated the role of water in the water-swollen hydrogel CO_2-selective membranes [15]. However, little information about the

* Corresponding author. Tel.: +47 73594033; fax: +47 73594080.
  E-mail address: hagg@nt.ntnu.no (M.-B. Hägg).

feed gas relative humidity effects on swelling behavior or on gas permeation properties of this type of hydrogel membrane is available. Reports on the swelling–relative humidity relationship could hardly be found; most studies on hydrogel swelling behavior were conducted in aqueous solutions, not in humidified gas environments.

This paper focuses on an experimental study and analysis of the swelling behavior of the PVAm/PVA blend membrane with respect to the effect of relative humidity and the influences of operating parameters on permeation of CO_2 and other gases. One of the most important findings of this investigation is that there are two stages of swelling in the PVAm/PVA blend membrane, which have been confirmed by the best fit of two exponential functions to the experimental results and is believed to be the evidence for a reversible, humidity-induced phase transition. The effects of operating parameters in CO_2/N_2 and CO_2/CH_4 mixed gas separation and CO_2, O_2, N_2, H_2, CH_4 single gas permeation were documented, including pressure, temperature, CO_2 concentration and flow rate of the feed gas.

2. Experimental

The PVAm/PVA blend composite membrane was synthesized with a thin homogenous blend selective layer (0.3–0.7 μm) on a PSf ultrafiltration membrane (Alfa Laval, MWCO 50,000). The blend solution was prepared by mixing PVA solution (90+% hydrolyzed powder, MW 72,000) and PVAm solution (Polyscience, Inc., MW 25,000) with a PVAm content of 80%. The blend polymer solution was homogenized overnight and sonicated with ultrasound for 2–10 min to ensure a molecular level mixing of the two polymers. The solution was filtered with a 0.25 μm syringe filter, and then cast onto a PSf substrate by dip-coating, using a procedure for ultra-thin membrane casting developed in this study. A thin and continuous solution layer was formed after casting the solution evenly on the membrane support, which was then fixed vertically on a glass plate to let any surplus solution flow off. An equilibrium thickness was obtained after water evaporated [16]. This procedure was repeated 2 or 4 times by alternately fixing the glass plate from up and down sides to reduce the thickness difference. Therefore, the thickness of this coating layer can be determined by the concentration of the casting solution and the number of times used for coating. Nevertheless, the selective layer thickness of the membranes was measured from the cross-section SEM images using FESEM (Zeiss Ultra 55 Limited Edition). All membranes were dried in an oven at 45 °C for 5 h and then cross-linked by heating at 105 °C for 1 h in a convection oven. The samples for the swelling study were heat cross-linked at the same condition as that of the membranes previously reported [14], in which the heat cross-linking of the PVAm and PVA chains also was documented by using FT-IR, XPS and XRD spectra — these are therefore not included here.

Separation performance of membranes was tested in a mixed gas permeation rig as reported in [14]. A flat sheet membrane (diameter of 50 mm) was mounted in a flat type membrane module with a porous metal disk as the support. A bypass for dry feed gas with a precise valve parallel to humidified feed gas stream was designed to adjust the relative humidity of the separation system. The entire system was placed in a temperature-controlled chamber to prevent condensation of water in the membrane module. Flow rate and pressure were recorded and controlled by the flow controller, flow indicator and pressure transmitters (MKS), respectively, and logged directly into a computer (by Labview). Relative humidity of the separation system was measured by recording the relative humidity of the retentate gas directly from the membrane cell using a humidity analyzer and Rotronic HygroData HTS HW3 program. The compositions of the retentate

1. Humidifier 2. Buffer bottle 3. Membrane module
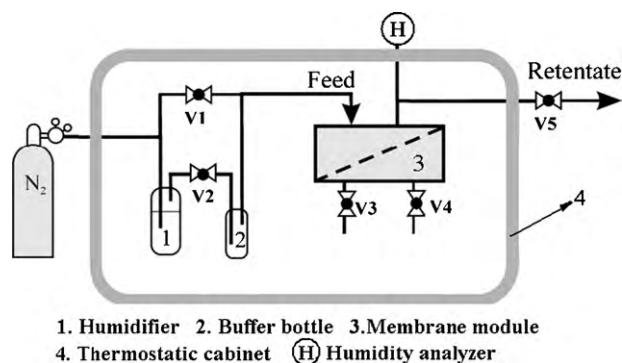4. Thermostatic cabinet (H) Humidity analyzer

Fig. 1. Experimental set-up for swelling test at controlled relative humidity.

and permeate streams were determined by a gas chromatograph (MicroGC3000) equipped with a thermal conductivity detector (TCD) and a "Plot Q" column. The permeation rate was measured by a bubble-flow-meter and the retentate flow rate was measured by a float-type-flow-meter. Pre-mixed feed gas and sweep gas were saturated with water vapor by passing it through a water humidifier before being feed into the membrane module. In mixed gas separation, CO_2 concentration in feed gas was 10 vol.% except those otherwise indicated.

Since the membranes in this study were highly water swollen in work condition and hence hard to determine the exact membrane selective layer thickness, the membrane permeation characteristics were evaluated by measuring the total CO_2 permeance of the composite membrane. Permeance of gas i is defined as the pressure-normalized flux of the gas through a membrane in units of $m^3(STP)/(m^2\,h\,bar)$ given the symbol P_i. The selectivity (α) was calculated from the ratio of permeance of CO_2 over CH_4, as expressed in Eq. (2):

$$P_i = \frac{J_i}{\Delta p_i} = \frac{q_{p,i}}{A \times \Delta p_i} \qquad (1)$$

$$\alpha = \frac{P_{CO_2}}{P_{CH_4}} \qquad (2)$$

where J_i represents the flux of component i in the unit of $m^3(STP)/(m^2\,h)$, Δp_i is the trans-membrane partial pressure difference (bar) and $q_{p,i}$ is the permeate flow rate of component i, in $m^3(STP)/h$, while A is the effective membrane area, m^2.

The swelling degree of the PVAm/PVA blend film sample was tested using the same membrane cell and relative humidity adjusting system as in the permeation test. The permeate side lines of the cell were closed (valves 3 and 4 as shown in Fig. 1). Nitrogen with a controlled relative humidity was feed at a pressure only slightly higher than the atmospheric pressure to ensure a driving force for a defined gas flow on the feed-retentate side. Other operating conditions such as temperature (25 °C) and feed flow rate (2.0 ml/s) were kept similar to those for the membrane permeation tests. The samples were weighed at different relative humidity. The weight of the samples was recorded when the relative humidity had been constant for 3 h and hence an equilibrium water uptake was reached (indicated by the humidity analyzer, H, in Fig. 1), while the dry samples were weighed after being conditioned in dry N_2 flow overnight. The difference between the masses of the humidified samples and the dry samples gave the mass of the water uptake of the swollen membrane. When testing the effect of swelling time, the dry samples were conditioned in a glass vessel saturated with water vapor at room temperature and weighed regularly over 7 days. The water swelling degree (SD) of membrane was calculated according to Eq.
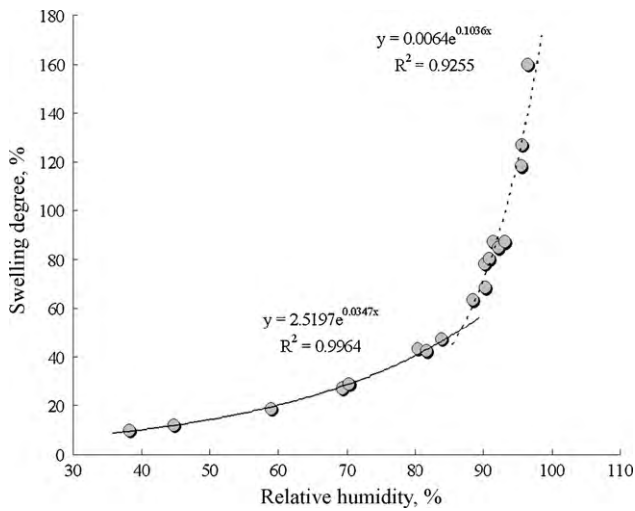
Fig. 2. Swelling characteristic of the PVAm/PVA blend film at room temperature.

(3).

$$SD(\%) = \frac{W_s - W_d}{W_d} \times 100 \tag{3}$$

where W_s and W_d are the mass of the swollen and dry membrane materials, respectively.

3. Results and discussion

3.1.1. Membrane swelling characteristic

With the unique hydrogel feature and CO_2 facilitated transport mechanism, PVAm/PVA blend FSC membranes exhibit both high CO_2 permeance and selectivity at high relative humidity. In addition, a very strong dependence of the CO_2 permeation on relative humidity of the operating system has been found from the experimental results, which can be easily related to the phenomenon that the swelling behavior of this membrane depends on the relative humidity, or substantially, the amount of water moisture in feed gases. In order to reveal the influence of relative humidity on the membrane separation performance, the swelling behavior of membrane was investigated.

The swelling degree of the PVAm/PVA blend sample was plotted as a function of the relative humidity in Fig. 2. The swelling degree of the sample exponentially increased with the relative humidity increasing, with two exponential functions in different ranges (solid line and dashed line, respectively), exhibiting a clear biphasic behavior. The curve fitting equations and their respective correlation coefficient (R^2) are expressed in the figure. In the relative humidity range 30–85%, R^2 value for the regression of the experimental data as the first exponential function is around 0.996, implying the highly satisfactorily fitting for the experimental data. Deviation from the first exponential equation becomes great when the relative humidity excesses a certain transition point, which is believed to be the critical relative humidity for the swelling of the PVAm/PVA blend sample. The swelling process exhibits two distinguished stages with relative humidity being lower or higher than this critical point. The experimental data in the higher relative humidity range (>85%) can be expressed in another function. It could be an exponential function as shown in the figure, but it is more likely to be a combination of an exponential function and a polynomial function according to the general dependence of the polymer swelling on the amount of the solvent, as suggested by some swelling theories in [17].

The basic and most known theory for polymer swelling study may be the Flory–Huggins theory. According to the Flory–Huggins theory, the swelling free energy for mixing (ΔG_m) is attributed to two entropy factors; one due to the conformations of polymer molecules ($\Delta G_{conform}$), and the other due to the contact between polymer segments and solvent molecules ($\Delta G_{contact}$). For the water swelling in cross-linked hydrogel case, the free energy contributions can be expressed in Eqs. (4) and (5), respectively [17]:

$$\Delta G_{conform} = RT[\ln \phi_w + \phi_p] \tag{4}$$

$$\Delta G_{contact} = RT\chi\phi_p^2 \tag{5}$$

where R is the gas constant, T is absolute temperature, ϕ is the volume fraction, ρ is density, χ is the polymer–solvent interaction parameter. The subscript w represents water and p is polymer, respectively.

In the low relative humidity range, the swelling is in the conformation determining stage, where ($\Delta G_{conform}$) and terms in Eq. (4) contributes more to the overall swelling. In this stage, the structural relaxation is induced by the mixing of the solvent water with the polymer chains. Swelling degree growth was limited and depended largely on the water content in the gas phase, hence exhibiting a clear exponential dependence on relative humidity. The second stage starts when the relative humidity is above a critical point, then the swelling of the polymer becomes contact-controlling, and hence the effects of term ($\Delta G_{contact}$) and the factors in Eq. (5) becomes significant, the overall swelling process is then determined by the combination of the conformation and contact factors. In this stage, the swelling is affected by the water affinity of the polymer and depends more on the amount of the water presented in the system, thus the swelling degree increased dramatically with a slightly increase of the relative humidity. Swelling degree increases as relative humidity increase in this process, and the swelling reaches equilibrium if the free energy for mixing, ΔG_m, equals to that for the polymer network deformation (opposite of the elastic free energy, represented as $-\Delta G_e$), as expressed in Eqs. (6) and (7) [18].

$$\Delta G_e = RT\left(\frac{\rho_p \widetilde{V}_s}{\overline{M}c}\right)\phi_p^{1/3} \tag{6}$$

$$RT[\ln \phi_w + \phi_p] + RT\chi\phi_p^2 + RT\left(\frac{\rho_p \widetilde{V}_s}{\overline{M}c}\right)\phi_p^{1/3} = 0 \tag{7}$$

where $\widetilde{V}_s$ is the molar volume of solvent and $\overline{M_c}$ is the molecular mass of the network chain. Eq. (7) is the swelling equilibrium equation, which indicates the effects of the environments and the polymer network properties that determine the swelling conditions. Although it is not yet possible to theoretically predict the swelling of the blended PVAm/PVA membrane due to the lack of detailed data for the blend polymer network structure (e.g. $\overline{M_c}$, χ), the Flory–Huggins theory confirms the general exponential dependence of the swelling degree on relative humidity and the two stage (biphasic) swelling behavior: the empirical relationships based on experiments. These could be a reliable guideline to the determining of the optimal relative humidity for the CO_2 separation process using swelling FSC membranes.

According to experiments, the operation pressure, or more precisely, the pressure difference throughout the membrane, exhibited strong influence on membrane performance. Higher pressure difference (at 2–15 bar) generally resulted in lower gas permeance. This is believed to result from the pressure induced swelling capacity decreasing due to the compacting of the membrane network under pressure. From the stability point of view, however, this phenomenon is beneficial, since the compacting effect may effectively restrict the polymer network deformation caused by the
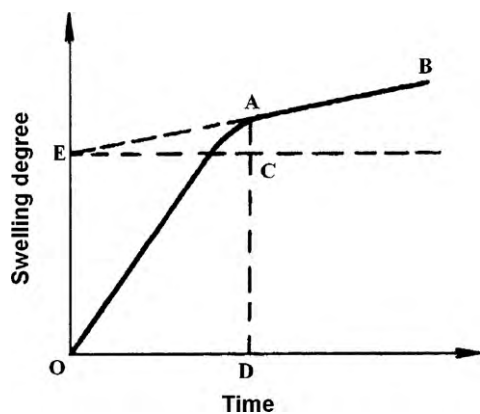
Fig. 3. Typical swelling curve for cross-linked polymer [18].

Fig. 4. Swelling–time curves of PVAm/PVA blend and PVA samples at room temperature, 100% relative humidity.

extra swelling expansion. An approx. 400 h test for CO_2/N_2 separation in [14] can provide a piece of evidence for the stability of this blend membrane for gas separation applications.

Experiments also showed that the time used to reach the stable separation performance varied for different membranes, and it was found generally depended on the membrane materials and the membrane preparation conditions. There are several kinetic models to evaluate swelling of hydrogels at the time basis that may explain this phenomenon and give a rough estimation of the stabilizing time for the PVAm/PVA blend membrane [19–23]. A typical swelling–time curve of a cross-linked polymer in solvent as a function of swelling time is illustrated in Fig. 3 [18]. The swelling degree increases very fast in the beginning of the swelling process (marked as OA), while the growth of the swelling degree decreased after a certain time when the swelling degree reaches the maximum physical swelling degree (marked as E on the y-coordinate). Further increasing of the swelling degree on time is nearly linear at a small slope, suggesting that the swelling equilibrium is not yet reached. The swelling growth in this stage, shown as CA, is the additional swelling growth caused by the broken of network. In this stage, the mobility of the chains becomes less restricted, and hence the polymer matrix network becomes weak, which may result in the loss of the membrane sieving capability. Since the swelling of the PVAm/PVA membrane is expected to be reversible and the cross-linked structure to be able to restore to the initial state, the swelling stage marked as CA is preferred not to take place.

Swelling–time curve of PVAm/PVA blend sample in a water saturated environment at room temperature is given in Fig. 4. The swelling data for PVA was also included in the figure for comparison. As shown in the graphs, the maximum physical swelling degrees of the PVAm/PVA blend and PVA were approximately 175% and 75%, respectively. To control the swelling of the PVAm/PVA blend membrane lower than 175% is hence very important for a long term stability of the membrane, therefore the relative humidity for the membrane separation system using the blend membrane should be less than 98.5% according to the swelling–relative humidity relationship.

A simple analysis using the second order equation, as expressed in Eq. (8) [23], is adapted to evaluate the equilibrium swelling degree of the PVAm/PVA blend membrane with the swelling–time curve. The integrated Eq. (8) over the limits $S = S_0$ at $t = t_0$ and $S = S$ at $t = t$, gives Eq. (9).

$$\frac{dS}{dt} = k_S(S_{eq} - S)^2 \tag{8}$$

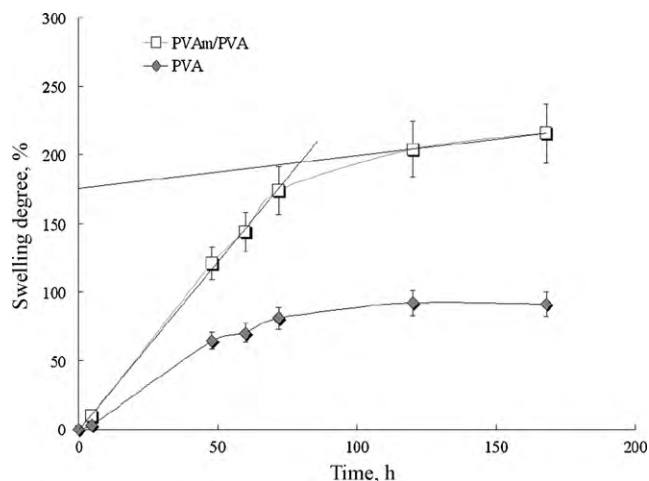$$\frac{t}{S} = \frac{1}{k_S S_{eq}^2} + \left(\frac{1}{S_{eq}}\right)t \tag{9}$$

where S_{eq} denotes the theoretical equilibrium swelling degree, S, swelling degree at time t, and k_S, the swelling rate constant. To examine the above kinetic model for the PVAm/PVA blend samples, t/S versus t graphs were plotted in Fig. 5 based on data from the swelling–time curve shown in Fig. 4, and the swelling rate constant (k_S) and theoretical equilibrium swelling (S_{eq}) values of the blend were calculated from the linear equations. As the slope of the equation for the PVAm/PVA membrane is 0.0033 ($1/S_{eq}$), the equilibrium swelling (theoretical) of the membrane in humidified gas flow was approximately 300%, and that for PVA around 110% (from $1/S_{eq} = 0.009$). The swelling rate constant (k_S) for PVAm/PVA blend could be calculated to be approximately 5×10^{-5} (g gel/g water)/h, and that for PVA is 2.9×10^{-4} (g gel/g water)/h, implying that it is almost 6 times faster for PVA to reach swelling equilibrium.

3.1.2. Effect of relative humidity on gas permeation

The influence of relative humidity on the membrane separation performance was investigated through mixed gas and single gas permeation tests. The experimental results of CO_2/CH_4 and CO_2/N_2 mixed gas separation are shown in Fig. 6 with relative humidity varying from 40% to 95%. The plots of CO_2 permeance as a function of relative humidity exhibit clear exponential trends, as expressed
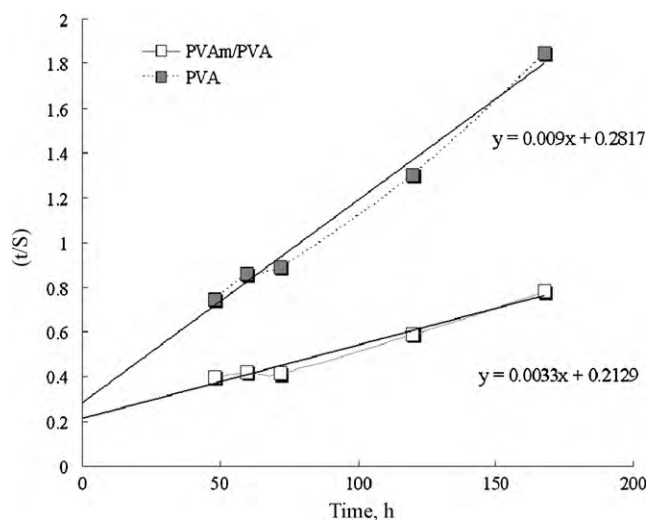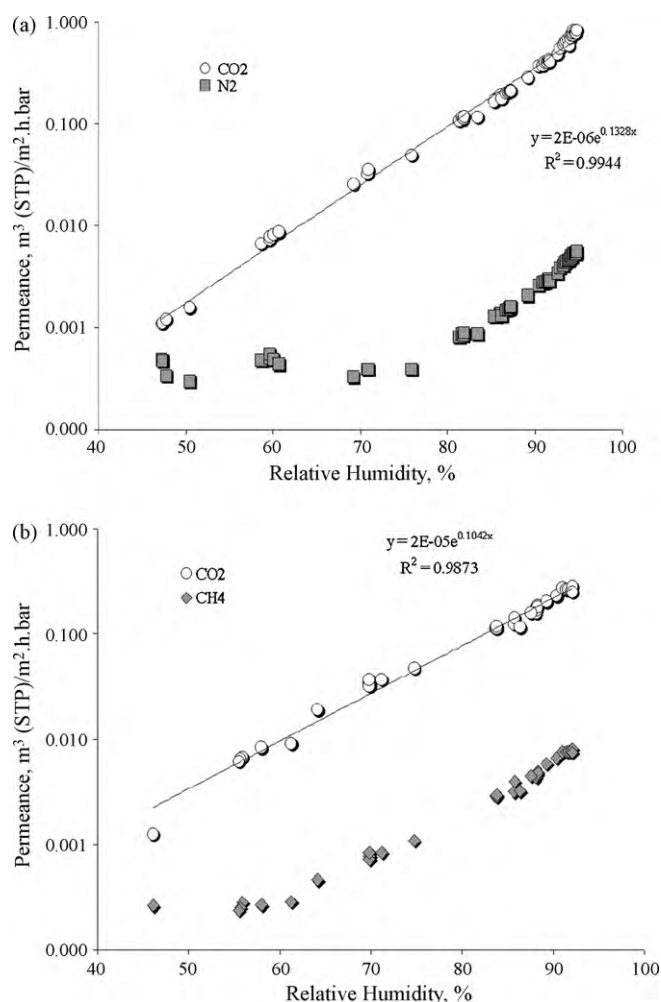

Fig. 5. Time/swelling degree (t/S) as a function of time (t) for PVAm/PVA blend and PVA swelling data.
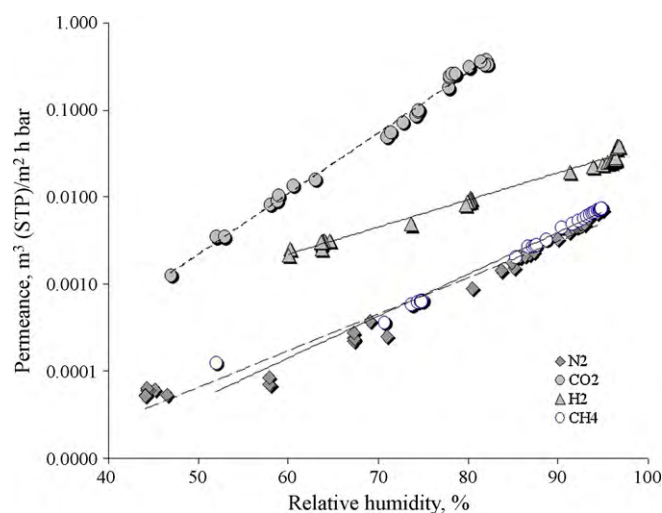
Fig. 6. Effect of relative humidity of feed gas on (a) CO_2 and N_2 permeances and (b) CO_2 and CH_4 permeances in mixed gas separations (CO_2 10 vol.%), at 2 bar, 25 °C.

Fig. 7. CO_2, CH_4, N_2, H_2 permeances in single gas tests, at 2 bar, 25 °C.

in the regression equations in Fig. 6(a) and (b), and the correlation coefficients of the regressions R^2 are both around 0.99. The exponential growth of CO_2 permeance with relative humidity increasing suggested that high relative humidity favors CO_2 transport, and the higher the relative humidity is, the more sensitive the CO_2 permeance growth to the relative humidity fluctuation. In addition, experiments showed an obviously higher CO_2 permeance in CO_2–N_2 separation than that in CO_2–CH_4 separations. The CO_2 permeance up to 0.83 m³(STP)/(m² h bar) was obtained for CO_2–N_2 separation while only 0.35 was reached for CO_2–CH_4 separation with the same membrane. Besides, the permeances of CO_2 in mixed gas tests and single gas tests are remarkably different. This phenomenon suggests that the influence from CH_4 is stronger than that from N_2 may be due to the higher CH_4 solubility in water than that of N_2 and CH_4 (with larger size) may hinder the diffusions of CO_2 and HCO_3^- more than N_2 does.

Single gas tests were conducted to study the permeation without gas interactions. The permeation data of gas CO_2, CH_4, N_2 and H_2 are plotted as a function of relative humidity in Fig. 7. The curve fittings for each permeation data are included in the figure, which seem all in good fittings of exponential functions. The plots of CH_4 and N_2 permeance in the single gas tests (see Fig. 7) are found different from those in CO_2–N_2 and CO_2–CH_4 mixed gas tests, which also confirmed the gas interactions during the permeation. The plot of CO_2 permeance in single gas test is above the plots of that in mixed gas CO_2–N_2 and CO_2–CH_4 tests shown in Fig. 6.

However, the CO_2 permeance of the single CO_2 only reached 0.37 at the maximum relative humidity around 83%, much lower than that in mixed CO_2–N_2 gas test, which reached a CO_2 permeance of 0.83 m³(STP)/(m² h bar) at the relative humidity of 95% (see Fig. 6). The phenomenon that lower maximum relative humidity reached in the single gas test may be explain by the higher consumption of water for the CO_2 facilitated transport through the membrane for higher CO_2 concentration in single gas permeation.

Regression analysis on experimental results indicates an empirically exponential relationship with different pre-exponential factor A_0 and constant B assigned to different gases, as expressed in Eq. (10), where Y represents the CO_2 permeance, m³(STP)/(m² h bar), and x is the relative humidity (%). The A_0 and B data for each gas are listed in Table 1, which can be determined from the slope (=B) and the intercept (ln A_0) of the plots in the natural logarithm y-coordinate. Since the gas permeance is in an exponential growth on relative humidity, the B value influences more on the overall permeance, especially at high relative humidity range. It is therefore important to improve the B value to achieve high CO_2 permeance and selectivity.

$$Y = A_0 \exp(Bx) \tag{10}$$

According to the experiments, the pre-exponential factor (A_0) may differ at different operating temperature and size of gases; factors which may influence gas transport through dry membranes. Constant B in the exponential equation, however, shows the sensitivity of the separation performance on relative humidity, which may depend more on the interaction between gas, water and membrane matrix, including the solubility of gas in water and reaction of gas and water facilitating the gas diffusion. Matsuyama et al. proposed a diffusion model with a normalized diffusion coefficient for solute in PVA hydrogel membranes, which may partly explain the general influences of the above mentioned aspects on constants A_0

Table 1
A_0 and B data in permeation equations of gas CO_2, CH_4, N_2 and H_2 in a PVAm/PVA blend membrane.

Gas	A_0	B
CO_2	7×10^{-07}	0.16
CH_4	2×10^{-07}	0.11
N_2	5×10^{-07}	0.10
H_2	3×10^{-05}	0.07
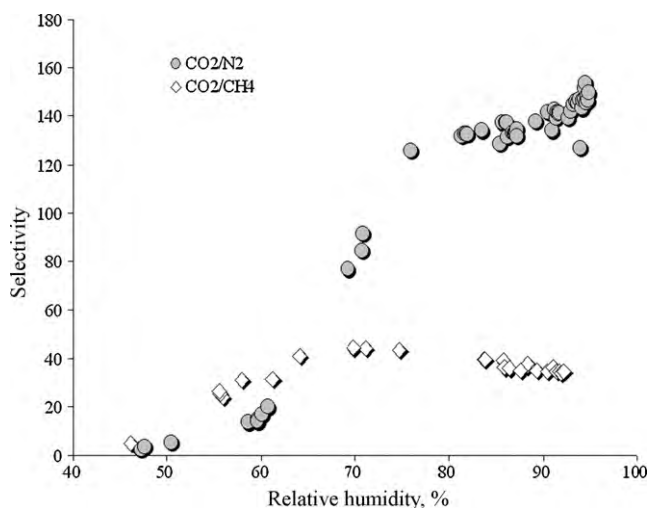
Fig. 8. Selectivity of CO_2/CH_4 and CO_2/N_2, at 25 °C, 2 bar.

Fig. 9. SEM cross-section image of a double dip-coated PVAm/PVA blend membrane.

and B [24]:

$$\left(\frac{D_{gel}}{D_{water}} \right) = K' \exp\left(-\frac{\pi r_s^2 l(1/H - 1)}{V_1} \right) \quad (11)$$

here r_s is the Stokes hydrodynamic radius, l is the characteristic length, V_l is the average free volume of the gel, H is the volume fraction of water in gel membrane. The partition coefficient, K', denotes the probability of a diffusing species finding a mesh formed by the cross-linked chains of the polymeric network, and depends on the size and shape of the mesh formed by the cross-linked chains and the size and concentration of the solute. According to this model, the influence by K' and V_l, which reflects the solute affinity and hydrogel cross-link condition, may be accounted for by the pre-exponential factor A_0, while r_s, l, H, etc., which stands for the solute size, membrane thickness and swelling degree, may affect the diffusion, reflected by the exponential constant B. Nevertheless, the determination of the mentioned constants and characteristic parameters is beyond the scope of this study, therefore the influences of the gas and membrane characteristics on the permeance–relative humidity relationship were not able to be quantitively analyzed for each gas at specified conditions; only a general trend could be provided in the current stage.

Fig. 8 presents the experimental results of the selectivity of CO_2/CH_4 and CO_2/N_2 obtained from the mixed gas tests. Generally, CO_2 selectivity increases with the increasing relative humidity, while in CO_2/CH_4 separation a slight selectivity drop occurred when relative humidity reached a certain point. The selectivity drop at high relative humidity range may be explained by the two stage swelling phenomenon. The second stage swelling of membrane at high relative humidity may cause the loosening of membrane structure and hence reduce the sieving capacity to CH_4, resulting in the loss of selectivity. Although the selectivity of CO_2/N_2 does not decrease with the increase of the relative humidity, the growth rate of the selectivity in the high relative humidity range dramatically reduces, probably also due to the second stage swelling in the membrane. The CO_2/N_2 selectivity in Fig. 8 (range in selectivity: 5–160) shows a decrease compared to the results previously published in [14] (selectivity range there was 65–174) although the selective layer thickness of the two membranes are similar — this decrease could be a result of the change in the membrane casting procedures. With the solvent being vertically evaporated and double coated during casting, it is believed that the new casting procedure used in the current work can result in a different microstructure with a denser and more even coating compared
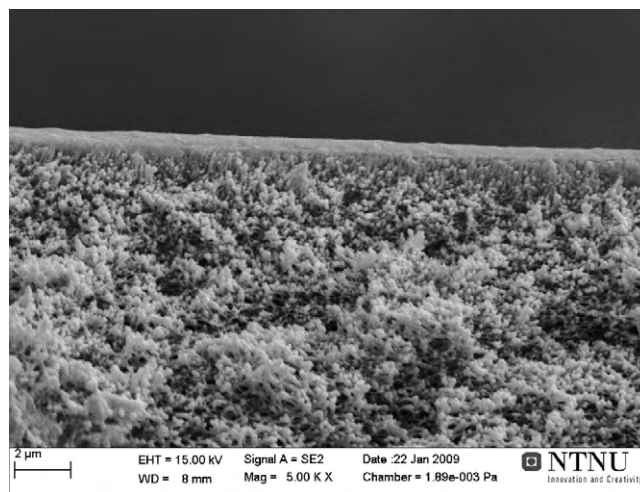
with the previously reported solution casting procedure in [14]. The SEM images of the cross-section of the membrane prepared by double dip-coating is given in Fig. 9, showing an evidently denser and more smooth coating layer with much few defects, which is believed to result from the double coating and vertically evaporating. The defects formed in the first coating are easily covered by the second coating, and hence hardly any defects through the membrane could occur. In low relative humidity range before defects in the membrane are able to be cured by swelling expansion, gas transport through the coating layer is mainly through the defects, therefore the solution cast membrane (with more defects) shows much higher gas permeance. In addition, the amino groups on the wall of these paths benefit the transport of CO_2 by facilitated selective surface diffusion, giving an enhanced selectivity, which may explain why in the low relative humidity range, the solution cast membrane also exhibits higher selectivity than membranes made by dip-coating. Since relative humidity <60% was not considered to be in the interesting range for a potential application, this difference in performance was not taken into account in membrane optimization. Detailed discussion about the two different membrane casting procedures has been presented in a subsequent paper concerning the optimization of membrane preparation conditions and will not be included in this paper.

4. Conclusion

In the current work, it was documented that hydrogel membranes with unique CO_2 facilitated transport fixed-site-carriers, such as PVAm/PVA blend membrane, exhibited much higher CO_2 permeance in the swollen state than the FSC membranes working in dry states. The interactions between gases strongly affect the gas separation. In separation of 10% CO_2 from $CO_2–N_2$ mixture, CO_2 permeance up to 0.83 m³(STP)/(m² h bar) and selectivity up to 160 were obtained at relative humidity 95%, while in separation of 35% CO_2 from $CO_2–CH_4$ mixture, CO_2 permeance up to 0.55 m³(STP)/(m² h bar) and selectivity up to 45 were obtained at relative humidity 92%.

A clear exponential dependence of swelling on relative humidity and the two stage swelling process were found in this study. The CO_2 permeance also shows an exponential growth on relative humidity increasing, indicating that the relative humidity has the most significant influence on CO_2 permeance. The gas permeation through this FSC membrane is complicated. Gas permeation depends not only on the diffusion of gas or dissolved solutes in the swollen membrane, but also on the solubility and the com-

plexation reactions between the gas, water and the membrane matrix. Some of the operation parameters, such as the pressure, flow rate and CO_2 concentration in feed, influence the separation performance, and are found partly through their respective influence on the relative humidity of the system. The theoretic analysis in this study confirmed the empirical relationships between relative humidity, swelling behavior and permeation properties of the PVAm/PVA blend membrane based on experimental results, which may provide the fundamental knowledge for the optimization of operating parameters and the practical applications of this type of FSC membranes.

Acknowledgements

References

[1] P.F. Scholander, Oxygen transport through hemoglobin solution, Science 131 (1960) 585.
[2] R.D. Noble, Relationship of system properties to performance in facilitated transport systems, Gas Separation & Purification 2 (1988) 16–19.
[3] R.D. Noble, J.D. Way, L.A. Powers, Effect of external mass-transfer resistance on facilitated transport, Industrial & Engineering Chemistry Fundamentals 25 (1986) 450–452.
[4] O.H. LeBlanc, W.J. Ward, S.L. Matson, S.G. Kimura, Facilitated transport in ion-exchange membranes, Journal of Membrane Science 6 (1980) 339–343.
[5] T.J. Kim, B.A. Li, M.B. Hagg, Novel fixed-site-carrier polyvinylamine membrane for carbon dioxide capture, Journal of Polymer Science Part B – Polymer Physics 42 (2004) 4326–4336.
[6] C.M. Xiao, G.Y. Zhou, Synthesis and properties of degradable poly(vinyl alcohol) hydrogel, Polymer Degradation and Stability 81 (2003) 297–301.
[7] B. Smitha, S. Sridhar, A.A. Khan, Synthesis and characterization of poly(vinyl alcohol)-based membranes for direct methanol fuel cell, Journal of Applied Polymer Science 95 (2005) 1154–1163.
[8] J.S. Park, J.W. Park, B.H. Kim, Thermomechanical characteristics of poly(vinyl alcohol)/chitosan films and its blend hydrogels, Polymer-Korea 29 (2005) 183–189.
[9] H. Matsuyama, A. Terada, T. Nakagawara, Y. Kitamura, M. Teramoto, Facilitated transport of CO_2 through polyethylenimine/poly(vinyl alcohol) blend membrane, Journal of Membrane Science 163 (1999) 221–227.
[10] M. Krumova, D. López, R. Benavente, C. Mijangos, J.M. Pereña, Effect of crosslinking on the mechanical and thermal properties of poly(vinyl alcohol), Polymer 41 (2000) 9265–9272.
[11] K.J. Kim, S.B. Lee, N.W. Han, Effects of the degree of cross-linking on properties of poly(vinyl alcohol) membranes, Polymer Journal 25 (1993) 1295–1302.
[12] H.J. Chun, S.B. Lee, S.Y. Nam, S.H. Ryu, S.Y. Jung, S.H. Shin, S.I. Cheong, J.W. Rhim, Preparation and swelling behavior of thermally cross-linked poly(vinyl alcohol) and poly(acrylic acid) hydrogel, Journal of Industrial and Engineering Chemistry 11 (2005) 556–560.
[13] Z. Wang, M. Li, Y. Cai, J. Wang, S. Wang, Novel CO_2 selectively permeating membranes containing PETEDA dendrimer, Journal of Membrane Science 290 (2007) 250–258.
[14] L. Deng, T.-J. Kim, M.-B. Hägg, Facilitated transport of CO_2 in novel PVAm/PVA blend membrane, Journal of Membrane Science 340 (2009) 154–163.
[15] L. Liu, A. Chakma, X. Feng, Gas permeation through water-swollen hydrogel membranes, Journal of Membrane Science 310 (2008) 66–75.
[16] M. Mulder, Basic Principles of Membrane Technology, 2nd ed., Kluwer Academic Publishers Inc., Netherland, 2003.
[17] P. Bahadur, N.V. Sastry, Principles of Polymer Science, Alpha Science International Ltd., Pangbourne, 2002.
[18] Q. Wu, Y. Feng, Introduction to High Polymer Material (in Chinese), China Machine Press, Beijing, 2004, p. 169.
[19] W.-L. Chen, K.R. Shull, T. Papatheodorou, D.A. Styrkas, J.L. Keddie, Equilibrium swelling of hydrophilic polyacrylates in humid environments, Macromolecules 32 (1998) 136–144.
[20] T. Çaykara, I. Akçakaya, Synthesis and network structure of ionic poly(N,N-dimethylacrylamide-co-acrylamide) hydrogels: comparison of swelling degree with theory, European Polymer Journal 42 (2006) 1437–1445.
[21] K. Ralf, S. Johannes, K. Wolfgang, The swelling behavior of polyelectrolyte multilayers in air of different relative humidity and in water, Macromolecular Chemistry and Physics 203 (2002) 413–419.
[22] J.B. Donald, B. Martin, P. Dennis, The swelling of polymer systems in solvents. I. Method for obtaining complete swelling–time curves, Journal of Polymer Science 56 (1962) 163–174.
[23] Y.M. Mohan, P.S.K. Murthy, J. Sreeramulu, K.M. Raju, Swelling behavior of semi-interpenetrating polymer network hydrogels composed of poly(vinyl alcohol) and poly(acrylamide-co-sodium methacrylate), Journal of Applied Polymer Science 98 (2005) 302–314.
[24] H. Matsuyama, M. Teramoto, H. Urano, Analysis of solute diffusion in poly(vinyl alcohol) hydrogel membrane, Journal of Membrane Science 126 (1997) 151–160.